J. Fluid Mech. (1983), *vol.* 131, *pp.* 1–26
Printed in Great Britain

The spreading of a liquid on a rough solid surface

By R. G. COX

Pulp and Paper Research Institute of Canada and Department of Civil Engineering and Applied Mechanics, McGill University, Montreal, Canada

(Received 23 October 1980 and in revised form 12 January 1983)

The equilibrium configurations of a liquid spreading on a rough solid surface are derived by making expansions in terms of the characteristic slope ϵ of the surface roughness, which is assumed to be very small. It is also assumed that the microscopic contact angle is a constant and that the liquid–air interface is planar at large distances from the contact line. Expressions for the value of the macroscopic contact angle and a discussion of the existence of contact-angle hysteresis and of stick-jump behaviour of the contact line are given for (i) surfaces with parallel grooves, (ii) surfaces with periodicity in two perpendicular directions and (iii) general non-period surfaces.

1. Introduction

It is known that the roughness of a solid surface has an important effect on the spreading of a liquid on that surface. For example, certain types of roughness can have a strong directional influence on spreading, as has been demonstrated qualitatively by Trillat & Fritz (1938), Parker & Smoluchowski (1945), Bikerman (1950), Bascom, Cottington & Singleterry (1964), Oliver & Mason (1977) and Oliver, Huh & Mason (1977). A simple relation between surface roughness and the value of the contact angle (defined as the angle between the solid–liquid and liquid–air interfaces) was derived by Wenzel (1936) using an energy-conservation argument. However, he assumed that the value of the contact angle was a constant independent of the motion of the contact line (defined as the line where the liquid–air and solid surfaces meet), whereas it is well known that for an advancing contact line the value of the contact angle is greater than that for a receding contact line. This phenomenon, known as contact-angle hysteresis, may result from the roughness of the surface or from variations in the chemical nature of the surface from one position to another. Johnson & Dettre (1964) and Huh & Mason (1977*a*) examined the possible axisymmetric equilibrium positions of a drop resting on a horizontal surface with roughness in the form of a series of concentric circular grooves. They showed that if the local microscopic contact angle (i.e. the angle between the local solid–liquid surface and liquid–air surface at the contact line) was taken to have a constant value α_0, then there are in general many possible equilibrium positions of the drop. They deduced that this would result in contact-angle hysteresis and also that the forward or receding motion of the contact line would not be steady as the drop volume was slowly increased or decreased. Instead the contact line would progress in a series of jumps in a stick–jump behaviour. The details of what happens during such a jump is not predicted by the theory since fluid-dynamical effects must be important during the actual jumping process as the drop passes through non-equilibrium configurations.

The question arises as to what happens when spreading occurs on more general types of rough planar surfaces. It is this which we will attempt to answer in the present paper. We will assume, as did Huh & Mason (1977*a*), that in the spreading

process the microscopic contact angle has a constant value α_0. However, in making this assumption it must be admitted that it is not known whether on a perfect surface which is flat and smooth and shows no chemical heterogeneity the contact angle takes a unique value. It has been suggested (Schwartz 1980) that an intrinsic contact-angle hysteresis may exist on even such perfect solid surfaces, while other authors (Huh & Mason 1977*a*) believe that no hysteresis would be evident should the maximum lengthscale of the roughness be less than some critical value. Whatever the true situation may be, the assumption of a constant microscopic contact angle is convenient for examining the effect of surface roughness.

As the contact line is made to move very slowly on the rough surface, we will calculate the possible equilibrium positions of the liquid–air surface and of the contact line. In particular, we calculate the value of the macroscopic contact angle β, defined as the angle between the mean solid surface position and the liquid–air interface at a distance far from the contact line where the liquid–air interface is assumed to be approximately planar. The way in which the values of this macroscopic contact angle varies with mean contact line position as it slowly advances or recedes may then be related to contact angle hysteresis and the stick–jump behaviour (Huh & Mason 1977*a*). Thus by finding only equilibrium positions we avoid the problem of the singularity in fluid flow stress which exists at a moving contact line even for spreading on a smooth solid surface (Dussan V. & Davis 1974; Hocking 1976, 1977; Huh & Mason 1977*b*; Dussan V. 1979).

Since it is very difficult to find the equilibrium shape of the liquid–air interface and the contact-line position for a general rough surface, we will assume that the characteristic surface slope ϵ of the roughness is small, and will make expansions in terms of this parameter. Huh & Mason (1977*a*) made this same assumption for a drop of fixed volume resting on a rough solid surface, but were unable to find more than one possible equilibrium position of the system. The reason for this, as will be explained in detail in the conclusion of the present paper, is due to the fact that for many possible equilibrium positions to exist we must have $\epsilon R \gg l$, where R^3 is the drop volume and l the characteristic wavelength of the surface roughness (i.e. the characteristic lengthscale of the roughness measured parallel to the surface). Thus, since Huh & Mason (1977*a*) considered the limit of $\epsilon \to 0$ with l/R fixed, this condition is violated and so only one equilibrium position can be found and there can be no possibility of contact-angle hysteresis. In the present paper, however, we consider the situation in which, at large distance from the contact line, the liquid–air interface becomes planar so that we are considering drops of infinite size for which l/R is zero. For such a case, the condition $\epsilon R \gg l$ is satisfied for any non-zero value of ϵ, however, small, so that many equilibrium positions can be expected.

The importance of an investigation into the effect of various types of surface roughness on the value of the macroscopic contact angle can be seen by considering spreading on a parallel grooved surfaced with surface elevation z given by

$$z = \epsilon A \sin \frac{2\pi x^*}{a} \tag{1.1}$$

where the rectangular coordinates (x^*, y^*) are defined parallel to the mean solid surface. When the contact line is parallel to the grooves (figure 1) the liquid–air interface is exactly planar so that the macroscopic contact angle β is therefore given by

$$\beta = \alpha_0 - \frac{\mathrm{d}z}{\mathrm{d}x^*} = \alpha_0 - \epsilon \frac{2\pi A}{a} \cos \frac{2\pi x_0^*}{a}, \tag{1.2}$$

where x_0^* is the value of x^* at the contact line.

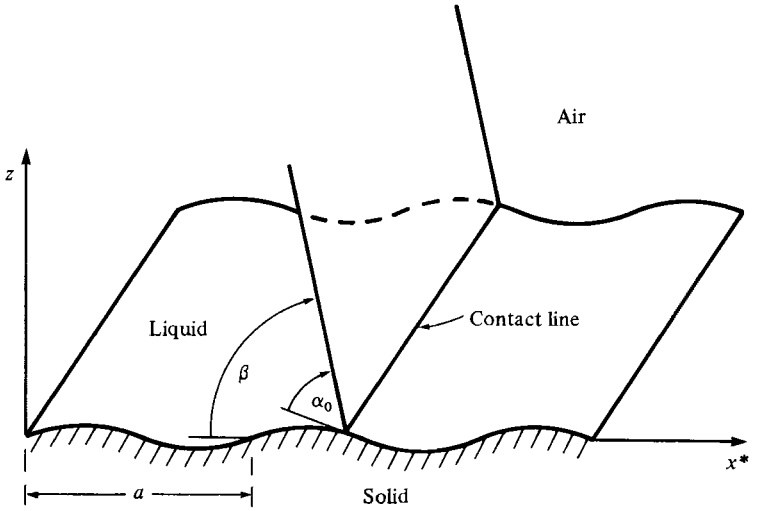

FIGURE 1. Liquid spreading on a solid surface with elevation z given as a function of position by (1.1). Contact line is parallel to the groove direction.

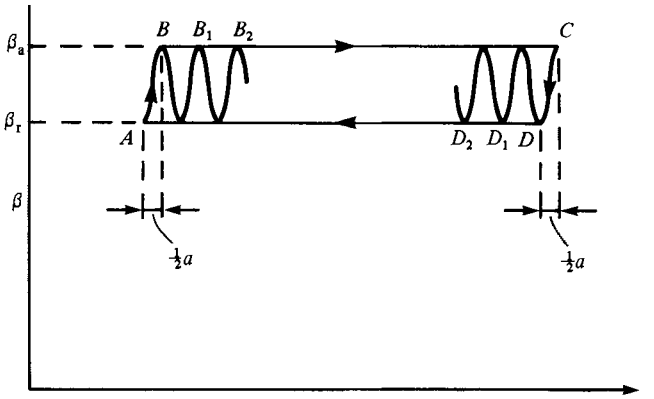

FIGURE 2. Value of macroscopic contact angle β as a function of contact-line position x_0^* for the spreading situation shown in figure 1.

Thus β is an oscillatory function of x_0^*, so that if the contact line is advanced by increasing the liquid volume (which means that β cannot decrease) then on the (x^*, β)-diagram shown in figure 2 we move from A to B with the contact angle increasing from $\beta_r = \alpha_0 - \epsilon(2\pi A/a)$ at A to $\beta_a = \alpha_0 + \epsilon(2\pi A/a)$ at B, while the contact line moves only a small distance $\frac{1}{2}a$. Since there is no equilibrium with $\beta > \beta_a$, the contact line jumps from B to B_1, sticks at B_1, then jumps from B_1 to B_2, etc. If at C the liquid volume is reduced, we move from C to D with β changing from β_a to β_r and the contact line only moving a small distance $\frac{1}{2}a$. At D there is a jump from D to D_1, where it sticks, followed by another jump from D_1 to D_2, etc. Thus we form the closed hysteresis loop $ABCDA$ with advancing and receding contact angles β_a and β_r respectively. Thus we have both contact-angle hysteresis and the stick–jump phenomenon similar to that described by Huh & Mason (1977*a*). However, when the contact line is in any direction other than parallel to the grooves, then each equilibrium position is seen to be geometrically the same as any other (see figure 3) so that the value of the macroscopic contact angle β would be independent of contact-line position, indicating no contact-angle hysteresis. Thus this example

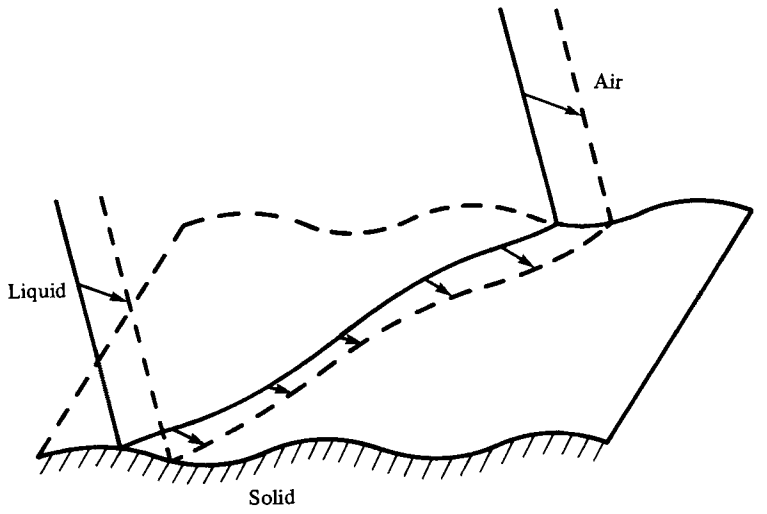

FIGURE 3. Liquid spreading on a solid surface with elevation z given by (1.1) and with the contact line making a non-zero angle with the groove direction.

illustrates that one can have surfaces that exhibit contact-angle hysteresis only for certain contact-line directions. It is of interest to know how general this type of behaviour is.

Thus, after describing the general theory in §2, we discuss in §3 spreading on surfaces for which there is periodicity along the contact line (such as would occur for the surface given by (1.1)). This is extended to spreading on surfaces with periodicity in two perpendicular directions in §4, and to surfaces with non-periodic roughness in §5. Finally, in §6 the connection between the results obtained and Wenzel's (1936) relation is discussed. In addition expressions are obtained for the energy released during any non-equilibrium jump of the contact line.

2. Theory

The spreading of a liquid on a rough solid planar surface is considered for the situation where the characteristic height h of the roughness is very much smaller than the roughness wavelength l (defined as the characteristic distance between roughness elements measured parallel to the surface). Thus, by taking a set of Cartesian axes (x', y', z') with the z'-axis perpendicular to the mean position of the solid surface (and directed away from the solid), the surface roughness of the solid may be expressed as

$$\frac{z'}{h} = \zeta\left(\frac{x'}{l}, \frac{y'}{l}\right). \tag{2.1}$$

Thus, if dimensionless coordinates (x, y, z) are defined using l as the characteristic lengthscale so that

$$x = \frac{x'}{l}, \quad y = \frac{y'}{l}, \quad z = \frac{z'}{l}, \tag{2.2}$$

the surface elevation given by (2.1) may be written as

$$z = \epsilon\zeta(x, y), \tag{2.3}$$

where ζ is of order unity and where the characteristic surface slope

$$\epsilon \equiv \frac{h}{l} \ll 1. \tag{2.4}$$

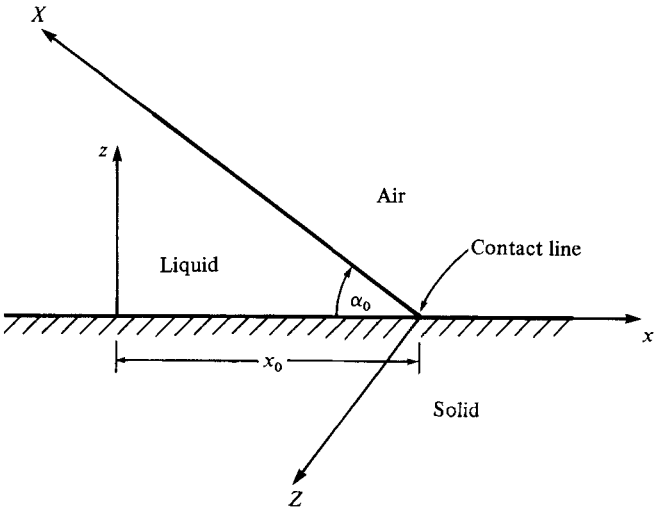

FIGURE 4. Definition of axes for spreading on a plane solid surface (for which $\epsilon = 0$).

We suppose that the liquid–air interface of the spreading liquid moves so slowly that the interface moves from one static equilibrium position to another. Furthermore, as mentioned in § 1, we assume that the liquid–air interface is planar at large distances and also that the contact angle between the solid and liquid–air interfaces at their line of intersection (the contact line) is a constant α_0. The value of this constant α_0 should differ from both 0 and π by an amount large compared with ϵ since otherwise the contact line will no longer be a single almost-straight line, there possibly being islands of solid surface appearing through the liquid–air interface.

When the solid is smooth (i.e. when $\epsilon = 0$) the liquid–air interface is a plane which makes an angle α_0 with the solid surface. Without loss of generality, we take the y-axis in the solid surface parallel to the contact line, which we suppose is at $x = x_0$ (see figure 4). A new dimensionless set of coordinates (X, Y, Z) is then defined with origin on the contact line $x = x_0$ and X-axis along the liquid–air interface perpendicular to the contact line. The Z-axis is then taken to be perpendicular to the liquid–air interface and directed into the liquid (so that the Y- and y-axes are then parallel). The (X, Y, Z)-coordinates are then related to the (x, y, z)-coordinates by the relations

$$\left.\begin{aligned} X &= -(x-x_0)\cos\alpha_0 + z\sin\alpha_0, \\ Y &= y, \\ Z &= -(x-x_0)\sin\alpha_0 - z\cos\alpha_0. \end{aligned}\right\} \tag{2.5}$$

For a rough solid surface for which ϵ is small but non-zero, we determine the position of the liquid–air interface as an expansion in terms of the small parameter ϵ as

$$Z = \epsilon f_1(X, Y) + \epsilon^2 f_2(X, Y) + \ldots. \tag{2.6}$$

There can be no terms in ϵ^0 in this expansion since as $\epsilon \to 0$ the liquid–air interface is expected to tend to $Z = 0$, the solution for the smooth surface. Since this liquid–air interface is assumed to tend to a planar surface at large distances (i.e. as $X \to \infty$), its equilibrium shape is such that the pressure difference across it is everywhere zero (assuming that the effect of gravity is negligible). Thus the liquid–air interface

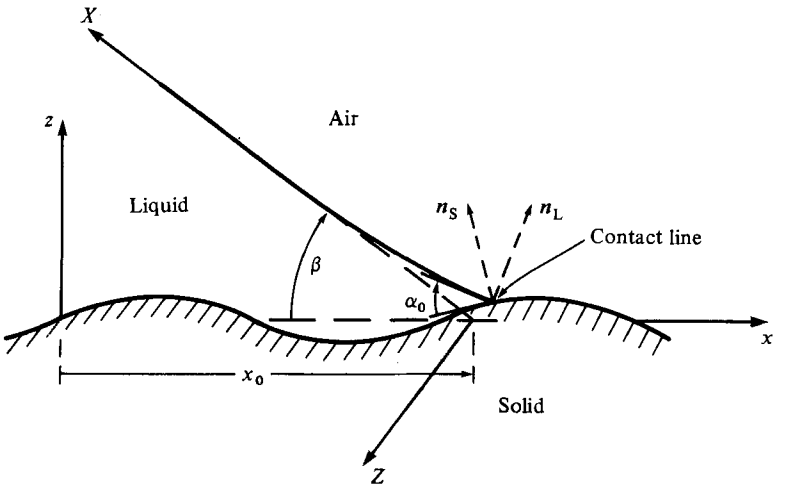

FIGURE 5. Definition of axes for spreading on a general rough solid surface. $\boldsymbol{n}_S$ and $\boldsymbol{n}_L$ are respectively the unit normals to the solid and liquid interfaces at the contact line. α_0 is the microscopic contact angle and β the macroscopic contact angle.

$Z = Z[X, Y]$ given by (2.6) must have zero curvature (i.e. zero invariant of the curvature tensor) for all X, Y, so that

$$\frac{1}{H}\left\{\frac{\partial^2 Z}{\partial X^2}+\frac{\partial^2 Z}{\partial Y^2}\right\}-\frac{1}{H^3}\left\{\left(\frac{\partial Z}{\partial X}\right)^2\frac{\partial^2 Z}{\partial X^2}+2\frac{\partial Z}{\partial X}\frac{\partial Z}{\partial Y}\frac{\partial^2 Z}{\partial X\,\partial Y}+\left(\frac{\partial Z}{\partial Y}\right)^2\frac{\partial^2 Z}{\partial Y^2}\right\}=0, \quad (2.7)$$

where

$$H=\left\{1+\left(\frac{\partial Z}{\partial X}\right)^2+\left(\frac{\partial Z}{\partial Y}\right)^2\right\}^{\frac{1}{2}}.$$

Substituting the expansion (2.6) into this equation and equating like powers of ϵ, we find that $f_1(X, Y)$ and $f_2(X, Y)$ satisfy

$$\frac{\partial^2 f_1}{\partial X^2}+\frac{\partial^2 f_1}{\partial Y^2}=0, \quad \frac{\partial^2 f_2}{\partial X^2}+\frac{\partial^2 f_2}{\partial Y^2}=0. \quad (2.8a, b)$$

At the contact line (see figure 5), where the solid surface (2.3) and liquid–air interface (2.6) intersect,

$$\begin{aligned}-(x-x_0)\sin\alpha_0-\epsilon\zeta(x,y)\cos\alpha_0 &= \epsilon f_1\{-(x-x_0)\cos\alpha_0+\epsilon\zeta(x,y)\sin\alpha_0, y\}\\ &\quad+\epsilon^2 f_2\{-(x-x_0)\cos\alpha_0+\epsilon\zeta(x,y)\sin\alpha_0, y\}+\ldots,\end{aligned} \quad (2.9)$$

where use has been made of the transformation (2.5). This equation (2.9) may be considered as giving the position x of the contact line for each value of y. Since the contact line is at $x = x_0$ when $\epsilon\to 0$, we assume the solution of (2.9) to be of the form

$$x = x_0+\epsilon g_1(y)+\epsilon^2 g_2(y)+\ldots. \quad (2.10)$$

By substituting this value of x into (2.9) and expanding $\zeta(x, y)$ in a Taylor series about $x = x_0$, we see, by equating like powers of ϵ, that $g_1(y)$ and $g_2(y)$ are

$$g_1(y) = -\frac{1}{\sin\alpha_0}f_1(0, y)-\cot\alpha_0\,\zeta(x_0, y), \quad (2.11)$$

$$g_2(y) = -\frac{1}{\sin\alpha_0} f_2(0,y) - \frac{1}{\sin^2\alpha_0}\{\zeta(x_0,y) + \cos\alpha_0 f_1(0,y)\}\frac{\partial f_1}{\partial X}(0,y)$$
$$+ \frac{\cos\alpha_0}{\sin^2\alpha_0}\{\cos\alpha_0\,\zeta(x_0,y) + f_1(0,y)\}\frac{\partial\zeta}{\partial x}(x_0,y). \quad (2.12)$$

The surface elevation z at the contact line is $\epsilon\zeta(x,y)$, where x is given by (2.10)–(2.12). Thus, by expanding this for small ϵ, we find that at the contact line

$$z = \epsilon h_1(y) + \epsilon^2 h_2(y) + \ldots, \quad (2.13)$$

where
$$h_1(y) = \zeta(x_0,y), \quad (2.14)$$

$$h_2(y) = -\frac{1}{\sin\alpha_0}\{f_1(0,y) + \cos\alpha_0\,\zeta(x_0,y)\}\frac{\partial\zeta}{\partial x}(x_0,y). \quad (2.15)$$

Since the contact angle is assumed to take the constant value α_0, it follows that

$$\boldsymbol{n}_S \cdot \boldsymbol{n}_L = \cos\alpha_0 \quad (2.16)$$

at all points on the contact line where $\boldsymbol{n}_S$ and $\boldsymbol{n}_L$ are unit normals to the solid and liquid–air surfaces respectively at the contact line, both directed towards the air (see figure 5).

The unit normal $\boldsymbol{n}_S$ to the solid surface (given by (2.3)) has components

$$(n_{Sx}, n_{Sy}, n_{Sz}) = \left[1 + \left(\epsilon\frac{\partial\zeta}{\partial x}\right)^2 + \left(\epsilon\frac{\partial\zeta}{\partial y}\right)^2\right]^{-\frac{1}{2}}\left(-\epsilon\frac{\partial\zeta}{\partial x}, -\epsilon\frac{\partial\zeta}{\partial y}, +1\right) \quad (2.17)$$

relative to the (x,y,z) axes, while in a similar manner the unit normal $\boldsymbol{n}_L$ to the liquid–air interface (given by (2.6)) has components

$$(n_{LX}, n_{LY}, n_{LZ}) = \left[1 + \left(\epsilon\frac{\partial f_1}{\partial X} + \epsilon^2\frac{\partial f_2}{\partial X} + \ldots\right)^2 + \left(\epsilon\frac{\partial f_1}{\partial Y} + \epsilon^2\frac{\partial f_2}{\partial Y} + \ldots\right)^2\right]^{-\frac{1}{2}}$$
$$\times\left(+\epsilon\frac{\partial f_1}{\partial X} + \epsilon^2\frac{\partial f_2}{\partial X} + \ldots, +\epsilon\frac{\partial f_1}{\partial Y} + \epsilon^2\frac{\partial f_2}{\partial Y} + \ldots, -1\right) \quad (2.18)$$

relative to the $(X,\ Y,\ X)$-axes. By expressing $\boldsymbol{n}_S$ in terms of this same set of axes and substituting into (2.16), we obtain the boundary condition for the liquid–air interface that is to be applied at the contact line at which for each value of y, x is given by (2.10)–(2.12) and z by (2.13)–(2.15). This boundary condition is then converted to one at the line $X = Z = 0$ (or $x = x_0, z = 0$) by expanding all quantities as Taylor series about this position. Thus, after a lengthy calculation, we obtain upon equating like powers of ϵ, the boundary conditions for f_1 and f_2 to be applied at $X = 0$ as

$$\left.\frac{\partial f_1}{\partial X}\right|_{X=0} = \frac{\partial\zeta}{\partial x}(x_0,y), \quad (2.19)$$

$$\left.\frac{\partial f_2}{\partial X}\right|_{X=0} = -\frac{1}{\sin\alpha_0}\left.f_1\right|_{X=0}\frac{\partial^2\zeta}{\partial x^2}(x_0,y) - \cot\alpha_0\,\zeta(x_0,y)\frac{\partial^2\zeta}{\partial x^2}(x_0,y)$$
$$-\cot\alpha_0\left.f_1\right|_{X=0}\left.\frac{\partial^2 f_1}{\partial X^2}\right|_{X=0} - \frac{1}{\sin\alpha_0}\zeta(x_0,y)\left.\frac{\partial^2 f_1}{\partial X^2}\right|_{X=0}$$
$$+\frac{1}{\sin\alpha_0}\frac{\partial\zeta}{\partial y}(x_0,y)\left.\frac{\partial f_1}{\partial Y}\right|_{X=0} + \tfrac{1}{2}\cot\alpha_0\left\{\frac{\partial\zeta}{\partial y}(x_0,y)\right\}^2 + \tfrac{1}{2}\cot\alpha_0\left\{\left.\frac{\partial f_1}{\partial Y}\right|_{X=0}\right\}^2. \quad (2.20)$$

Thus, for any rough solid surface for which $\zeta(x, y)$ is known, the shape of the liquid–air interface (2.6) for any x_0 is found to order ϵ by solving (2.8a) with boundary condition (2.19) and to order ϵ^2 by solving (2.8b) with boundary condition (2.20).

3. Roughness periodic along contact line

As an example we consider a rough solid surface in which the elevation $\zeta(x, y)$ is periodic with period b along the line $X = Z = 0$ (i.e. on $x = x_0$, $z = 0$), so that in the neighbourhood of the contact line $\zeta(x, y)$ may be expressed as the Fourier series

$$\zeta(x, y) = \sum_{n=1}^{\infty} \left\{ p_n(x) \sin \frac{2\pi n y}{b} + q_n(x) \cos \frac{2\pi n y}{b} \right\} + q_0(x). \tag{3.1}$$

It is therefore expected that the shape of the liquid–air interface would also be periodic in the Y-direction with period b. Thus $f_1(X, Y)$ in (2.6) must be periodic with period b whilst also satisfying (2.8a). It is therefore of the form

$$f_1(X, Y) = \sum_{n=1}^{\infty} \left\{ A_n \sin \frac{2\pi n Y}{b} + B_n \cos \frac{2\pi n Y}{b} \right\} \exp\left(- \frac{2\pi n X}{b} \right) + DX + E, \tag{3.2}$$

where $A_1, A_2, \ldots, B_1, B_2, \ldots, D$ and E are constants.

The term DX must be retained since we want to allow for the possibility of the macroscopic contact angle β (i.e. the angle between the liquid–air interface at $X \to \infty$ and the mean solid surface) being different from the value α_0 for a smooth surface. Since the liquid air–interface is given by (2.6) with f_1 determined by (3.2), it follows that to order ϵ^{+1},

$$\beta = \alpha_0 - \epsilon D + \ldots. \tag{3.3}$$

However, without loss of generality, we may take

$$E = 0 \tag{3.4}$$

by suitably defining the value of x_0 for each liquid–air interface (see figure 5). By substituting the values of ζ given by (3.1) and f_1 given by (3.2) into the boundary condition (2.19) and equating Fourier coefficients, we obtain the values of the unknown constants in the expression (3.2) for $f_1(X, Y)$. In this manner, the configuration of the liquid–air interface is obtained correct to order ϵ^{+1} as

$$Z = \epsilon \left[- \frac{b}{2\pi} \sum_{n=1}^{\infty} \frac{1}{n} \left\{ p_n'(x_0) \sin \frac{2\pi n Y}{b} + q_n'(x_0) \cos \frac{2\pi n Y}{b} \right\} \times \exp\left(- \frac{2\pi n X}{b} \right) + q_0'(x_0) X \right] + \ldots, \tag{3.5}$$

where primes denote differentiation with respect to x. The macroscopic contact angle is thus

$$\beta = \alpha_0 - \epsilon q_0'(x_0) + \ldots. \tag{3.6}$$

From the expression (3.1) for the surface elevation, it is observed that the value $\overline{(\partial\zeta/\partial x)}|_{x=x_0}$ of $\partial\zeta/\partial x$ averaged along the line $x = x_0$ is $q_0'(x_0)$, so that the macroscopic contact angle β may be expressed alternatively as

$$\beta = \alpha_0 - \epsilon \overline{\frac{\partial \zeta}{\partial x}}\bigg|_{x=x_0} + \ldots \tag{3.7}$$

If the values of $f_1(0, y)$ obtained from (3.2) and of $\zeta(x_0, y)$ obtained from (3.1) are substituted into the expression (2.11) for $g_1(y)$, the position of the contact line given by (2.10) is found correct to order ϵ^{+1} as

$$x = x_0 + \epsilon\Big[\sum_{n=1}^{\infty}\Big\{\Big(\frac{b}{2\pi n \sin\alpha_0}p_n'(x_0) - \cot\alpha_0\, p_n(x_0)\Big)\sin\frac{2\pi n y}{b} + \Big(\frac{b}{2\pi n\sin\alpha_0}q_n'(x_0) - \cot\alpha_0\, q_n(x_0)\Big)\cos\frac{2\pi n y}{b}\Big\} - q_0(x_0)\cot\alpha_0\Big] + \ldots. \quad (3.8)$$

In order to obtain the value of the macroscopic contact angle β correct to order ϵ^2, it is noted that since f_2 satisfies the same equation as f_1 (see (2.8)) and must be planar as $X \to \infty$, the form of f_2 must be the same as f_1, so that

$$f_2(X, Y) = \sum_{n=1}^{\infty}\Big\{P_n \sin\frac{2\pi n Y}{b} + Q_n\cos\frac{2\pi n Y}{b}\Big\}\exp\Big(-\frac{2\pi n X}{b}\Big) + RX, \quad (3.9)$$

where $P_1, P_2, \ldots, Q_1, Q_2, \ldots, R$ are constants. The value of the macroscopic contact angle is then

$$\beta = \alpha_0 - \epsilon q_0'(x_0) - \epsilon^2 R + \ldots. \quad (3.10)$$

From (3.9) it is observed that the value of R may be expressed as

$$R = \frac{1}{b}\int_0^b \frac{\partial f_2}{\partial X}\Big|_{X=0}\,\mathrm{d}Y, \quad (3.11)$$

which, from the boundary condition (2.31), may be written as

$$\begin{aligned} R = &-\frac{1}{b\sin\alpha_0}\int_0^b f_1|_{X=0}\,\frac{\partial^2\zeta}{\partial x^2}(x_0, y)\,\mathrm{d}y - \frac{\cot\alpha_0}{b}\int_0^b \zeta(x_0, y)\frac{\partial^2\zeta}{\partial x^2}(x_0, y)\,\mathrm{d}y \\ &- \frac{\cot\alpha_0}{b}\int_0^b f_1|_{X=0}\,\frac{\partial^2 f_1}{\partial X^2}\Big|_{X=0}\mathrm{d}y - \frac{1}{b\sin\alpha_0}\int_0^b \zeta(x_0, y)\frac{\partial^2 f_1}{\partial X^2}\Big|_{X=0}\mathrm{d}y \\ &+ \frac{1}{b\sin\alpha_0}\int_0^b \frac{\partial\zeta}{\partial y}(x_0, y)\frac{\partial f_1}{\partial Y}\Big|_{X=0}\mathrm{d}y + \frac{\cot\alpha_0}{2b}\int_0^b\Big\{\frac{\partial\zeta}{\partial y}(x_0, y)\Big\}^2\mathrm{d}y \\ &+ \frac{\cot\alpha_0}{2b}\int_0^b\Big\{\frac{\partial f_1}{\partial Y}\Big|_{X=0}\Big\}^2\mathrm{d}y. \end{aligned} \quad (3.12)$$

Substituting into this expression the values of ζ given by (3.1) and of f_1 given by (3.2) with the known values of the constants, and performing the integrations, we obtain after a lengthy but straightforward calculation

$$\begin{aligned} R = &-\tfrac{1}{4}\cot\alpha_0\sum_{n=1}^{\infty}\{(p_n')^2 + (q_n')^2\} + \frac{\pi^2}{b^2}\cot\alpha_0\sum_{n=1}^{\infty}\{n^2(p_n^2 + q_n^2)\} + \frac{b}{4\pi\sin\alpha_0} \\ &\times\sum_{n=1}^{\infty} n^{-1}(p_n' p_n'' + q_n' q_n'') - \tfrac{1}{2}\cot\alpha_0\sum_{n=1}^{\infty}(p_n p_n'' + q_n q_n'') - \cot\alpha_0(q_0 q_0''), \end{aligned} \quad (3.13)$$

where $p_n, p_n', p_n'', q_n, q_n', q_n''$ are all evaluated at $x = x_0$. Thus, from (3.10), it is seen that the macroscopic contact angle is

$$\begin{aligned} \beta = \alpha_0 - \epsilon q_0' + \epsilon^2\Big[&\tfrac{1}{4}\cot\alpha_0\sum_{n=1}^{\infty}\{(p_n')^2 + (q_n')^2\} \\ &- \frac{\pi^2}{b^2}\cot\alpha_0\sum_{n=1}^{\infty}\{n^2(p_n^2 + q_n^2)\} - \frac{b}{4\pi\sin\alpha_0}\sum_{n=1}^{\infty} n^{-1}(p_n' p_n'' + q_n' q_n'') \\ &+ \tfrac{1}{2}\cot\alpha_0\sum_{n=1}^{\infty}(p_n p_n'' + q_n q_n'') + \cot\alpha_0(q_0 q_0'')\Big] + O(\epsilon^3). \end{aligned} \quad (3.14)$$

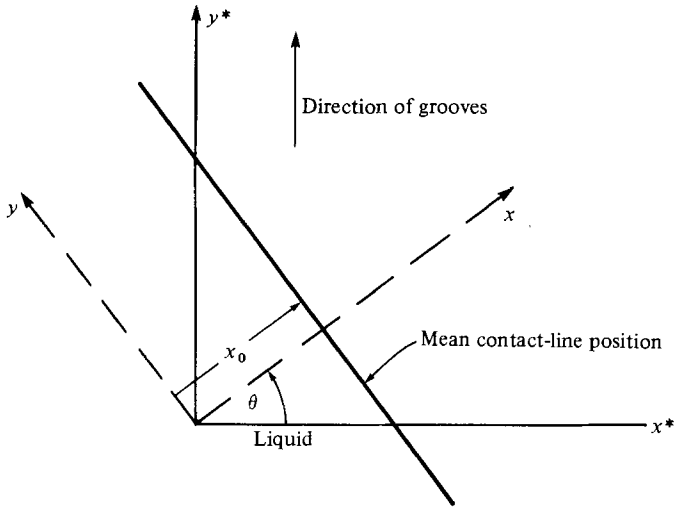

FIGURE 6. Definition of axes (x, y) and (x^*, y^*) in the plane of the rough solid surface. The liquid side of the contact line is to the lower left.

As a specific example of a surface for which $\zeta(x, y)$ near the contact line is of the form (3.1), consider a sinusoidal parallel grooved surface with

$$\zeta = A \sin \frac{2\pi x^*}{a} \tag{3.15}$$

relative to a fixed set of coordinates (x^*, y^*, z), where x^*, y^* lie in the surface, with the y^* axis parallel to the grooves. Then if the mean contact line makes an angle θ with the groove direction, and if (x, y, z)-axes are chosen as before with the y-axis parallel to the mean contact-line position $x = x_0$, it is observed that (see figure 6)

$$\left.\begin{aligned} x^* &= x\cos\theta - y\sin\theta, \\ y^* &= x\sin\theta + y\cos\theta. \end{aligned}\right\} \tag{3.16}$$

Thus, by substituting into (3.15), we obtain

$$\zeta = A \sin\left(\frac{2\pi\cos\theta}{a}x\right)\cos\left(\frac{2\pi\sin\theta}{a}y\right) - A\cos\left(\frac{2\pi\cos\theta}{a}x\right)\sin\left(\frac{2\pi\sin\theta}{a}y\right). \tag{3.17}$$

This, when compared with (3.1) with $b = a/\sin\theta$, gives for $\theta \neq 0$

$$p_1(x) = -A\cos\left(\frac{2\pi\cos\theta}{a}x\right), \quad q_1(x) = -A\sin\left(\frac{2\pi\cos\theta}{a}x\right), \tag{3.18}$$

with all other $p_n(x)$ and $q_n(x)$ zero; and for $\theta = 0$

$$q_0(x) = A\sin\left(\frac{2\pi}{a}x\right), \tag{3.19}$$

with all other $p_n(x)$ and $q_n(x)$ zero.

When the mean contact line position is not parallel to the grooves (i.e. when $\theta \neq 0$) the value of the macroscopic contact angle given by (3.14) is

$$\beta = \alpha_0 - \frac{\epsilon^2 A^2 \pi^2}{a^2}\cot\alpha_0 + O(\epsilon^3), \tag{3.20}$$

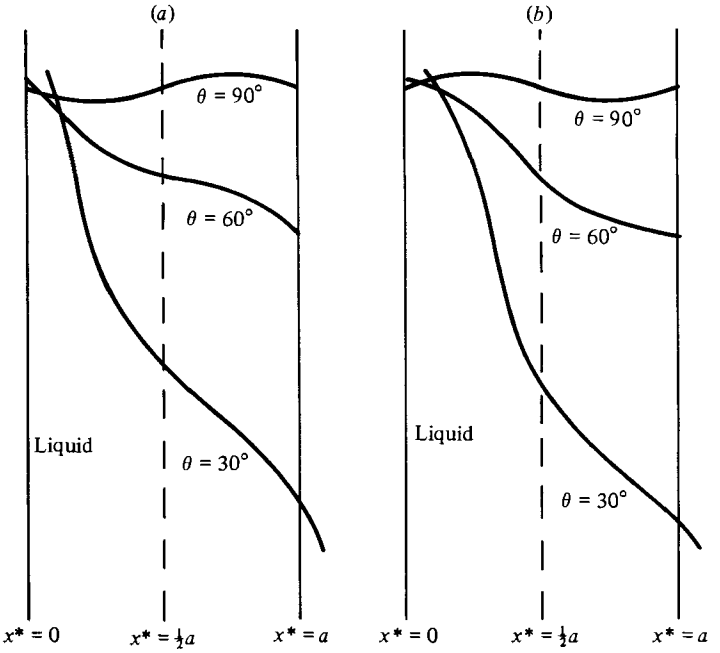

FIGURE 7. Contact-line positions (projected in the (x^*, y^*)-plane) for the surface with dimensionless elevation ζ given by (3.15) with $\epsilon A/a$ chosen to be 0.0278. For (*a*) the microscopic contact angle $\alpha_0 = 30°$, while for (*b*) $\alpha = 150°$. Situations for which the mean contact-line orientations are $\theta = 30°$, 60° and 90° have been plotted. The liquid side of the contact lines is to the lower left.

while the contact-line position to order ϵ^{+1}, determined by (3.8), may be expressed as

$$x = x_0 - \epsilon A \frac{(\cot^2\theta + \cos^2\alpha_0)^{\frac{1}{2}}}{\sin\alpha_0} \sin\left\{\frac{2\pi x_0^*}{a} - \tan^{-1}\left(\frac{\cot\theta}{\cos\alpha_0}\right)\right\}, \tag{3.21}$$

where $x_0^* = x_0\cos\theta - y\sin\theta$ is the value of x^* at the mean contact-line position $x = x_0$. For $0 < \theta \leqslant \frac{1}{2}\pi$, the value of the function $\tan^{-1}$ appearing in (3.21) must be chosen to be in the interval $(0, \pi)$. From these results it is seen that the following hold.

(i) There is no contact-angle hysteresis or stick–jump phenomenon since β is independent of contact-line position (i.e. it does not depend on x_0). This result was to be expected since all contact-line positions are geometrically equivalent.

(ii) For a microscopic contact angle $\alpha_0 < 90°$ the value of the macroscopic contact angle β is independent of contact-line orientation θ and is less than that for a smooth surface by an amount of order ϵ^2. For $\alpha_0 > 90°$, however, the value of β is increased by an amount of order ϵ^2.

(iii) When the mean contact line is perpendicular to the grooves (i.e. $\theta = 90°$), the contact line advances ahead of its mean position in the troughs for $\alpha_0 < 90°$, but advanced ahead of its mean position at the crests for $\alpha_0 > 90°$. However, when the angle θ the contact line makes with the grooves is reduced, the positions of maximum contact-line advance move towards the points of maximum uphill slope of the solid (i.e. the points on the contact line where $\partial\zeta/\partial x$ is a maximum). This is true whether α_0 is smaller or larger than 90° and is illustrated in figure 7.

(iv) As $\theta \to 0$ (i.e. when the contact line is almost parallel to the grooves), the wavelength $a/\sin\theta$ of the contact-line shape tends to infinity. Since this is also the lengthscale of the disturbance along the liquid–air interface in the X-direction, it

follows that the smaller the value of θ, the farther away along the liquid–air interface from the contact line one must go before it becomes approximately planar.

(v) The amplitude of the contact-line shape also tends to infinity (being $\approx \epsilon A \cot\theta \approx \epsilon A/\theta$) as $\theta \to 0$. Since for the validity of the theory this must be very much smaller than the lengthscale a of the solid-surface roughness, we require

$$\theta \gg \epsilon A/a, \tag{3.22}$$

which implies that θ must be much larger than the maximum slope angle of the roughness.

When the contact line is parallel to the grooves (i.e. when $\theta = 0$), so that $p_n(x)$ and $q_n(x)$ are given by (3.19), the value of the macroscopic contact angle given by (3.14) is

$$\beta = \alpha_0 - \epsilon \frac{2\pi A}{a} \cos\left(\frac{2\pi}{a} x_0\right) + O(\epsilon^2), \tag{3.23}$$

while the contact-line position (given by (3.8)) is

$$x = x_0 - \epsilon A \cot\alpha_0 \sin\left(\frac{2\pi}{a} x_0\right) + O(\epsilon^2). \tag{3.24}$$

Thus we observe for this case $\theta = 0$ that the following hold.

(i) There is contact-angle hysteresis to order ϵ^{+1}, with the advancing contact angle β_a being the maximum value of β, namely

$$\beta_a = \alpha_0 + \epsilon \frac{2\pi A}{a}, \tag{3.25}$$

and the receding contact angle β_r being the minimum value of β, namely

$$\beta_r = \alpha_0 - \epsilon \frac{2\pi A}{a}. \tag{3.26}$$

(ii) The stick-jump phenomenon will occur, with forward jumps at $(2\pi/a)\, x_0 = (2r+1)\,\pi$ for an advancing contact line, and receding jumps occurring at $(2\pi/a)\, x_0 = 2r\pi$ for a receding contact line (r is any integer).

(iii) The contact line is straight, as one would expect.

These results are in agreement with the remarks made in the introduction concerning this case.

4. Doubly periodic rough surfaces

From the results obtained in §3, it is observed that the behaviour and movement of a contact line on a parallel grooved solid surface is very much dependent on its orientation relative to the grooves. In order to see how general this type of situation is, we now investigate spreading of a liquid on a solid surface which is periodic with period a in the x^* direction and periodic with period b in the y^* direction so that $\zeta(x^*, y^*)$ may be expressed by the double Fourier series

$$\zeta = \sum_{m=0}^{\infty} \sum_{n=0}^{\infty} \left\{ a_{mn} \sin\frac{2\pi m x^*}{a} \sin\frac{2\pi n y^*}{b} + b_{mn} \sin\frac{2\pi m x^*}{a} \cos\frac{2\pi n y^*}{b} + c_{mn} \cos\frac{2\pi m x^*}{a} \sin\frac{2\pi n y^*}{b} + d_{mn} \cos\frac{2\pi m x^*}{a} \cos\frac{2\pi n y^*}{b} \right\}, \tag{4.1}$$

in which, by a suitable choice of origin of the (x^*, y^*, z)-coordinates, one may take $d_{00} = 0$ and therefore omit the case $m = n = 0$ from the double summation. In terms of the (x, y, z)-coordinates used previously, this value of ζ, by the use of (3.16), may be written as

$$\zeta = \sum_{m=0}^{\infty}\sum_{n=0}^{\infty}\{P_{mn}(x)\sin 2\pi\psi_{mn}y + Q_{mn}(x)\cos 2\pi\psi_{mn}y + \hat{P}_{mn}(x)\sin 2\pi\hat{\psi}_{mn}y + \hat{Q}_{mn}(x)\cos 2\pi\hat{\psi}_{mn}y\}, \quad (4.2)$$

where

$$\left.\begin{aligned} P_{mn}(x) &= \tfrac{1}{2}(a_{mn}+d_{mn})\sin 2\pi\hat{\chi}_{mn}x - \tfrac{1}{2}(b_{mn}-c_{mn})\cos 2\pi\hat{\chi}_{mn}x,\\ Q_{mn}(x) &= \tfrac{1}{2}(a_{mn}+d_{mn})\cos 2\pi\hat{\chi}_{mn}x + \tfrac{1}{2}(b_{mn}-c_{mn})\sin 2\pi\hat{\chi}_{mn}x,\\ \hat{P}_{mn}(x) &= -\tfrac{1}{2}(-a_{mn}+d_{mn})\sin 2\pi\chi_{mn}x + \tfrac{1}{2}(b_{mn}+c_{mn})\cos 2\pi\chi_{mn}x,\\ \hat{Q}_{mn}(x) &= \tfrac{1}{2}(-a_{mn}+d_{mn})\cos 2\pi\chi_{mn}x + \tfrac{1}{2}(b_{mn}+c_{mn})\sin 2\pi\chi_{mn}x, \end{aligned}\right\} \quad (4.3)$$

and

$$\left.\begin{aligned} \psi_{mn} &= \frac{m\sin\theta}{a} + \frac{n\cos\theta}{b}, \quad \hat{\psi}_{mn} = -\frac{m\sin\theta}{a} + \frac{n\cos\theta}{b},\\ \chi_{mn} &= \frac{m\cos\theta}{a} + \frac{n\sin\theta}{b}, \quad \hat{\chi}_{mn} = \frac{m\cos\theta}{a} - \frac{n\sin\theta}{b}. \end{aligned}\right\} \quad (4.4)$$

The value of the macroscopic contact angle β for a mean contact-line position at $x = x_0$ may be determined for this surface in a manner analogous to that discussed in §3 for a surface with a periodic variation along the contact line with ζ given by (3.1). Thus, in the present case, we take the value of f_1 to be

$$f_1(X, Y) = \sum_{m=0}^{\infty}\sum_{n=0}^{\infty}[\{A_{mn}\sin 2\pi\psi_{mn} + B_{mn}\cos 2\pi\psi_{mn}Y\}\exp(-2\pi|\psi_{mn}|X) + \{\hat{A}_{mn}\sin 2\pi\hat{\psi}_{mn}Y + B_{mn}\cos 2\pi\hat{\psi}_{mn}Y\}\exp(-2\pi|\hat{\psi}_{mn}|X)] + DX, \quad (4.5)$$

with $f_2(X, Y)$ given by a similar expression. In repeating the analysis of §3 for this situation, care must be exercised since certain cases, for which ζ and f_1 take special forms, must be examined separately. These exceptional cases are as follows.

(*a*) Values of θ for which

$$\tan\theta = \pm\frac{Na}{Mb}, \quad (4.6)$$

where N and M are positive integers ($\neq 0$), since there are then values of n and m for which either $\psi_{mn} = 0$ or $\hat{\psi}_{mn} = 0$.

(*b*) $\theta = 0$ and $\theta = \frac{1}{2}\pi$ for which $\psi_{mn} = \hat{\psi}_{mn}$ or $\psi_{mn} = -\hat{\psi}_{mn}$.

In addition, terms for which either $m = 0$ or $n = 0$ in the double sums in (4.2) and (4.4) must be considered separately (since these give $\psi_{mn} = \hat{\psi}_{mn}$ or $\psi_{mn} = -\hat{\psi}_{mn}$). Thus after a lengthy calculation, we obtain for the general case for which $\tan\theta \neq Na/Mb$ for any positive integers N and M (and $\theta \neq 0$ or $\frac{1}{2}\pi$), the value of the macroscopic contact angle β as

$$\beta = \alpha_0 - \tfrac{1}{2}\pi^2\epsilon^2\cot\alpha_0\left[\sum_{n=1}^{\infty}\frac{2n^2}{b^2}(c_{0n}^2+d_{0n}^2) + \sum_{m=1}^{\infty}\frac{2m^2}{a^2}(b_{m0}^2+d_{m0}^2) + \sum_{m=1}^{\infty}\sum_{n=1}^{\infty}\left(\frac{m^2}{a^2}+\frac{n^2}{b^2}\right)(a_{mn}^2+b_{mn}^2+c_{mn}^2+d_{mn}^2)\right], \quad (4.7)$$

with the contact-line position (to order ϵ^{+1}) being given by (2.10) with

$$g_1 = \frac{1}{\sin\alpha_0}\Bigg[\sum_{m=0}^{\infty}\sum_{n=0}^{\infty}(n^2a^2\cos^2\theta - m^2b^2\sin^2\theta)^{-1}\Bigg\{\begin{pmatrix}-(m^2b^2+n^2a^2)\sin\theta\cos\theta\\ mnab\end{pmatrix}$$
$$\times\Bigg(-c_{mn}\sin\frac{2\pi mx_0^*}{a}\sin\frac{2\pi ny_0^*}{b} - d_{mn}\sin\frac{2\pi mx_0^*}{a}\cos\frac{2\pi ny_0^*}{b} + a_{mn}\cos\frac{2\pi mx_0^*}{a}$$
$$\times\sin\frac{2\pi ny_0^*}{b} + b_{mn}\cos\frac{2\pi mx_0^*}{a}\cos\frac{2\pi ny_0^*}{b}\Bigg) + \begin{pmatrix}mnab\\ -(m^2b^2+n^2a^2)\sin\theta\cos\theta\end{pmatrix}$$
$$\times\Bigg(b_{mn}\sin\frac{2\pi mx_0^*}{a}\sin\frac{2\pi ny_0^*}{b} - a_{mn}\sin\frac{2\pi mx_0^*}{a}\cos\frac{2\pi ny_0^*}{b} + d_{mn}\cos\frac{2\pi mx_0^*}{a}$$
$$\times\sin\frac{2\pi ny_0^*}{b} - c_{mn}\cos\frac{2\pi mx_0^*}{a}\cos\frac{2\pi ny_0^*}{b}\Bigg)\Bigg\}\Bigg] - \cot\alpha_0\Bigg[\sum_{m=0}^{\infty}\sum_{n=0}^{\infty}\Bigg(a_{mn}\sin\frac{2\pi mx_0^*}{a}$$
$$\times\sin\frac{2\pi ny_0^*}{b} + b_{mn}\sin\frac{2\pi mx_0^*}{a}\cos\frac{2\pi ny_0^*}{b} + c_{mn}\cos\frac{2\pi mx_0^*}{a}\sin\frac{2\pi ny_0^*}{b} + d_{mn}$$
$$\times\cos\frac{2\pi mx_0^*}{a}\cos\frac{2\pi ny_0^*}{b}\Bigg)\Bigg]. \tag{4.8}$$

The upper and lower terms that appear in the expressions

$$\begin{pmatrix}-(m^2b^2+n^2a^2)\sin\theta\cos\theta\\ mnab\end{pmatrix},\quad \begin{pmatrix}mnab\\ -(m^2b^2+n^2a^2)\sin\theta\cos\theta\end{pmatrix}$$

are taken according to whether the value of n/m is less than or greater than $(b/a)\tan\theta$. The quantities x_0^* and y_0^* are the values of x^* and y^* respectively, evaluated on the mean contact-line position $x = x_0$, so that

$$x_0^* = x_0\cos\theta - y\sin\theta, \quad y_0^* = x_0\sin\theta + y\cos\theta. \tag{4.9}$$

For the particular situation where $\tan\theta = Na/Mb$, with N and M as positive integers, the values of β and g_1 may be obtained as

$$\beta = \alpha_0 - \frac{\epsilon\pi(N^2a^2+M^2b^2)^{\frac{1}{2}}}{ab}\Bigg[\sum_{p=1}^{\infty}p\Bigg\{(a_{rs}-d_{rs})\sin\frac{2\pi p(N^2a^2+M^2b^2)^{\frac{1}{2}}x_0}{ab}$$
$$+(b_{rs}+c_{rs})\cos\frac{2\pi p(N^2a^2+M^2b^2)^{\frac{1}{2}}x_0}{ab}\Bigg\}\Bigg] + O(\epsilon^2) \tag{4.10}$$

$$g_1 = \frac{1}{\sin\alpha_0}\Bigg[\sum_{m=0}^{\infty}\sum_{n=0}^{\infty}(n^2a^2\cos^2\theta - m^2b^2\sin^2\theta)^{-1}\Bigg\{\begin{pmatrix}-(m^2b^2+n^2a^2)\sin\theta\cos\theta\\ mnab\end{pmatrix}$$
$$\times\Bigg(-c_{mn}\sin\frac{2\pi mx_0^*}{a}\sin\frac{2\pi ny_0^*}{b} - d_{mn}\sin\frac{2\pi mx_0^*}{a}\cos\frac{2\pi ny_0^*}{b} + a_{mn}\cos\frac{2\pi mx_0^*}{a}$$
$$\times\sin\frac{2\pi ny_0^*}{b} + b_{mn}\cos\frac{2\pi mx_0^*}{a}\cos\frac{2\pi ny_0^*}{b}\Bigg) + \begin{pmatrix}mnab\\ -(m^2b^2+n^2a^2)\sin\theta\cos\theta\end{pmatrix}$$
$$\times\Bigg(b_{mn}\sin\frac{2\pi mx_0^*}{a}\sin\frac{2\pi ny_0^*}{b} - a_{mn}\sin\frac{2\pi mx_0^*}{a}\cos\frac{2\pi ny_0^*}{b} + d_{mn}\cos\frac{2\pi mx_0^*}{a}$$
$$\times\sin\frac{2\pi ny_0^*}{b} - c_{mn}\cos\frac{2\pi mx_0^*}{a}\cos\frac{2\pi ny_0^*}{b}\Bigg)\Bigg\} + \tfrac{1}{2}\cot 2\theta\sum_{p=1}^{\infty}\Big\{(a_{rs}+d_{rs})$$

$$\times \sin 2\pi p\left(-\frac{Mx_0^*}{a}+\frac{Ny_0^*}{b}\right)+(b_{rs}-c_{rs})\cos 2\pi p\left(-\frac{Mx_0^*}{a}+\frac{Ny_0^*}{b}\right)\Bigg\}\Bigg]$$

$$-\cot\alpha_0\Bigg[\sum_{m=0}^{\infty}\sum_{n=0}^{\infty}\left(a_{mn}\sin\frac{2\pi mx_0^*}{a}\sin\frac{2\pi ny_0^*}{b}+b_{mn}\sin\frac{2\pi mx_0^*}{a}\cos\frac{2\pi ny_0^*}{b}\right.$$

$$\left.+c_{mn}\cos\frac{2\pi mx_0^*}{a}\sin\frac{2\pi ny_0^*}{b}+d_{mn}\cos\frac{2\pi mx_0^*}{a}\cos\frac{2\pi ny_0^*}{b}\right)\Bigg], \tag{4.11}$$

where $r = pM$ and $s = pN$.

In the first double sum in (4.11) values of m and n for which $n/m = N/M$ are omitted, while the upper and lower terms in

$$\begin{pmatrix}-(m^2b^2+n^2a^2)\sin\theta\cos\theta\\ mnab\end{pmatrix},\quad\begin{pmatrix}mnab\\ -(m^2b^2+n^2a^2)\sin\theta\cos\theta\end{pmatrix}$$

are taken according to whether n/m is less than or greater than N/M.

The solution for the situation where $\tan\theta = -Na/Mb$ may be obtained by rotating the (x^*, y^*)-axes through $\frac{1}{2}\pi$ and using the above results (4.10) and (4.11). For the special case $\theta = 0$, the values of β and g_1 are

$$\beta = \alpha_0-\epsilon\sum_{m=1}^{\infty}\frac{2\pi m}{a}\left(b_{m0}\cos\frac{2\pi mx_0}{a}-d_{m0}\sin\frac{2\pi mx_0}{a}\right)+O(\epsilon^2), \tag{4.12}$$

$$g_1 = \frac{b}{a\sin\alpha_0}\sum_{m=1}^{\infty}\sum_{n=1}^{\infty}\frac{m}{n}\left(-c_{mn}\sin\frac{2\pi mx_0}{a}\sin\frac{2\pi ny}{b}-d_{mn}\sin\frac{2\pi mx_0}{a}\cos\frac{2\pi ny}{b}\right.$$

$$\left.+a_{mn}\cos\frac{2\pi mx_0}{a}\sin\frac{2\pi ny}{b}+b_{mn}\cos\frac{2\pi mx_0}{a}\cos\frac{2\pi ny}{b}\right)$$

$$-\cot\alpha_0\Bigg[\sum_{m=0}^{\infty}\sum_{n=0}^{\infty}\left(a_{mn}\sin\frac{2\pi mx_0}{a}\sin\frac{2\pi ny}{b}+b_{mn}\sin\frac{2\pi mx_0}{a}\cos\frac{2\pi ny}{b}\right.$$

$$\left.+c_{mn}\cos\frac{2\pi mx_0}{a}\sin\frac{2\pi ny}{b}+d_{mn}\cos\frac{2\pi mx_0}{a}\cos\frac{2\pi ny}{b}\right)\Bigg], \tag{4.13}$$

while the values for $\theta = \frac{1}{2}\pi$ may be obtained by rotating the (x, y) axes through an angle of $\frac{1}{2}\pi$. We now examine, in greater detail, two specific examples of spreading on a surface of the form (4.2).

Example (i). If $a = b$ and if the dimensionless surface elevation ζ contains only one Fourier coefficient, so that

$$\zeta = A\sin\frac{2\pi x^*}{a}\sin\frac{2\pi y^*}{a}, \tag{4.14}$$

then the value of the macroscopic contact angle (determined by (4.7), (4.10) and 4.12)) on such a surface is

$$\beta = \alpha_0-\epsilon^2\frac{\pi^2A^2}{a^2}\cot\alpha_0+O(\epsilon^3)\quad(0<\theta<\tfrac{1}{4}\pi), \tag{4.15}$$

$$\beta = \alpha_0-\epsilon\frac{\sqrt{2\pi}A}{a}\sin\frac{2\sqrt{2\pi}x_0}{a}+O(\epsilon^2)\quad(\theta=\tfrac{1}{4}\pi), \tag{4.16}$$

$$\beta = \alpha_0+\frac{\epsilon^2\pi^2A^2}{a^2}\left\{\cot\alpha_0\left(2\cos\frac{4\pi x_0}{a}-1\right)+\frac{1}{\sin\alpha_0}\cos\frac{4\pi x_0}{a}\right\}+O(\epsilon^3)\quad(\theta=0). \tag{4.17}$$

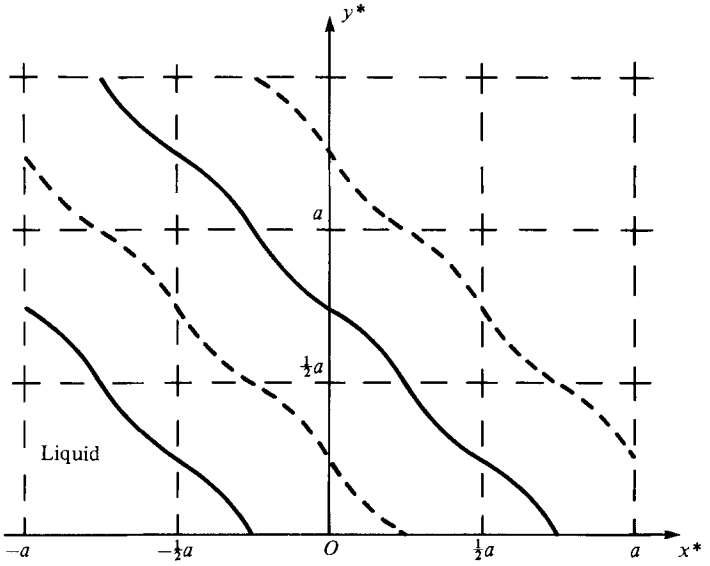

FIGURE 8. For spreading on a solid surface with dimensionless elevation ζ given by (4.14), the contact-line positions (projected in the (x^*, y^*)-plane) at which advancing jumps occur are shown by the continuous lines while those at which receding jumps occur are shown by broken lines. $\epsilon A/a$ has been chosen to be 0.025, while the microscopic contact angle α_0 has been taken to be 30°. The liquid side of the contact lines is to the lower left.

The term $O(\epsilon^2)$ in (4.17), while not being given by (4.12), was derived using (3.14). The contact-line position given by (4.8), (4.11) and (4.13) is found to be

$$x = x_0 + \epsilon A\left[\frac{1}{\sin\alpha_0\cos 2\theta}\left(\cos\frac{2\pi x_0^*}{a}\sin\frac{2\pi y_0^*}{a} + \sin 2\theta\sin\frac{2\pi x_0^*}{a}\cos\frac{2\pi y_0^*}{a}\right)\right.$$
$$\left. - \cot\alpha_0\sin\frac{2\pi x_0^*}{a}\sin\frac{2\pi y_0^*}{a}\right] + O(\epsilon^2) \quad (0 < \theta < \tfrac{1}{4}\pi), \tag{4.18}$$

$$x = x_0 - \epsilon A\cot\alpha_0\sin\frac{2\pi x_0^*}{a}\sin\frac{2\pi y_0^*}{a} + O(\epsilon^2) \quad (\theta = \tfrac{1}{4}\pi), \tag{4.19}$$

$$x = x_0 + \epsilon A\left\{\frac{1}{\sin\alpha_0}\cos\frac{2\pi x_0^*}{a}\sin\frac{2\pi y_0^*}{a} - \cot\alpha_0\sin\frac{2\pi x_0^*}{a}\sin\frac{2\pi y_0^*}{a}\right\} + O(\epsilon^2) \quad (\theta = 0). \tag{4.20}$$

Thus we observe that for spreading on this surface the following hold.

(*a*) There is no contact-angle hysteresis of order ϵ^{+1} except for $\theta = \frac{1}{4}\pi$ (and $\theta = -\frac{1}{4}\pi$), for which there is hysteresis of this order with advancing contact angle

$$\beta_a = \alpha_0 + \epsilon\frac{\sqrt{2\pi A}}{a} \tag{4.21}$$

and receding contact angle

$$\beta_r = \alpha_0 - \epsilon\frac{\sqrt{2\pi A}}{a}. \tag{4.22}$$

For $\theta = \frac{1}{4}\pi$, stick–jump behaviour occurs, with the jumps at $x_0 = \frac{1}{2}\sqrt{\frac{1}{2}a(\frac{3}{2}+2r)}$ for an advancing contact line and at $x_0 = \frac{1}{2}\sqrt{\frac{1}{2}a(\frac{1}{2}+2r)}$ for a receding contact line (where r is any integer). The exact position of the contact lines (to order ϵ^{+1}) at which these jumps occur (determined by (4.19)) are shown in figure 8. It is seen that the existance of hysteresis for $\theta = \frac{1}{4}\pi$ is due to the uneven ridges and valleys in the surface, which

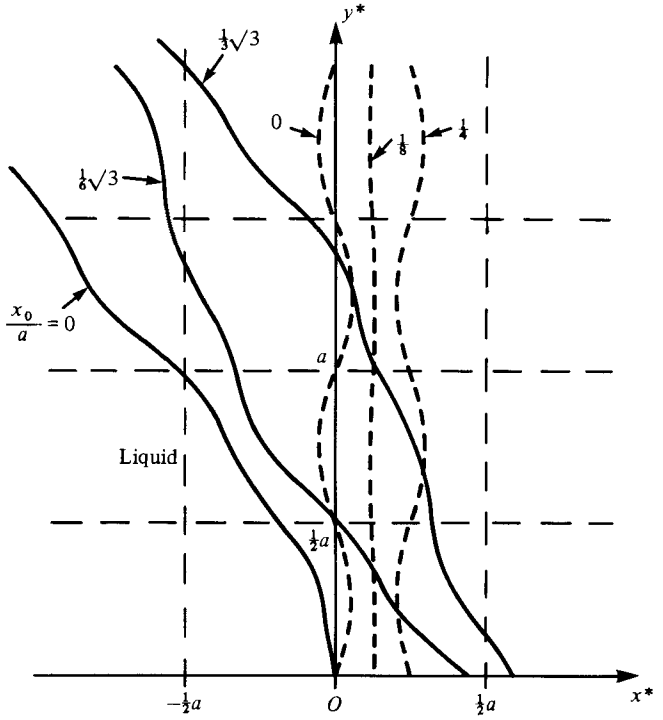

FIGURE 9. Other contact-line positions (projected in the (x^*, y^*)-plane) for the case shown in figure 8 (i.e. ζ given by (4.14) with $\epsilon A/a = 0.025$ and $\alpha_0 = 30°$). The continuous lines are for $\theta = 30°$ (with $x_0/a = 0$, $\frac{1}{8}\sqrt{3}$ and $\frac{1}{3}\sqrt{3}$) and the broken lines for $\theta = 0°$, (with $x_0/a = 0$, $\frac{1}{8}$ and $\frac{1}{4}$). The liquid side of the contact lines is to the left.

run parallel to the mean contact line when $\theta = \frac{1}{4}\pi$. It is also observed from (4.17) that there is also contact-angle hysteresis for $\theta = 0$ (and also for $\theta = \frac{1}{2}\pi$) but that this hysteresis is much smaller, being of order ϵ^2.

(*b*) When there is no contact-angle hysteresis (i.e. when $0 < \theta < \frac{1}{4}\pi$) the macroscopic contact angle is less than or greater than α_0 according to whether α_0 is less than or greater than $\frac{1}{2}\pi$. Such behaviour was also noted for the parallel grooved surface considered in §3 for $\theta \neq 0$.

(*c*) From the contact-line positions (correct to order ϵ^{+1}) given by (4.18) and shown in figure 9, it is observed that for $\alpha_0 < 90°$ the positions of maximum contact-line advance tend to occur where surface elevation ζ is a minimum and/or where surface upslope $\partial\zeta/\partial x$ is a maximum. This is the same as observed for the parallel grooved surface.

Example (ii). If $a = b$ and if the surface elevation ζ is given by the double Fourier sine series

$$\zeta = \sum_{m=1}^{\infty}\sum_{n=1}^{\infty} a_{mn} \sin\frac{2\pi m x^*}{a}\sin\frac{2\pi n y^*}{a}, \tag{4.23}$$

where in the area $0 \leqslant x^* \leqslant \frac{1}{2}a$, $0 \leqslant y^* \leqslant \frac{1}{2}a$, it represents the function

$$\zeta = \frac{A x^*(\frac{1}{2}a - x^*) y^*(\frac{1}{2}a - y^*)}{(\frac{1}{4}a)^4}, \tag{4.24}$$

then the Fourier coefficients a_{mn} may be determined, and we obtain

$$\zeta = \frac{1024A}{\pi^6}\sum_{r=0}^{\infty}\sum_{s=0}^{\infty}(2r+1)^{-3}(2s+1)^{-3}\sin\frac{2\pi(2r+1)x^*}{a}\sin\frac{2\pi(2s+1)y^*}{a}. \tag{4.25}$$

This surface is superficially similar to that given by (4.14) (with both having maximum and minimum values of $\pm A$ occurring at the same places), except that an infinite number of Fourier coefficients are now present. For spreading on this surface (4.25), the macroscopic contact angle β is found to be

$$\beta = \alpha_0 - \epsilon^2 \frac{512A^2}{45a^2} \cot \alpha_0 + O(\epsilon^3) \quad \text{if} \quad \tan\theta \neq \frac{2S+1}{2R+1}, \tag{4.26}$$

$$\beta = \alpha_0 + \epsilon \frac{2048A[(2R+1)^2+(2S+1)^2]^{\frac{1}{2}}}{15a(2R+1)^3(2S+1)^3} \bar{x}_0(\bar{x}_0-\tfrac{1}{2})(\bar{x}_0-1)(\bar{x}_0^2-\bar{x}_0-\tfrac{1}{3})$$
$$\text{if} \quad \tan\theta = \frac{2S+1}{2R+1}, \tag{4.27}$$

where
$$\bar{x}_0 = [(2R+1)^2+(2S+1)^2]^{\frac{1}{2}} x_0/a, \tag{4.28}$$

and R and S are integers $\geqslant 0$.

The result (4.27) is valid only for $0 \leqslant \bar{x} \leqslant 1$, the value of β outside of this range being determined by the fact that β is a periodic function of $\bar{x}_0$ with period unity.

In addition the contact-line position to order ϵ^{+1} is, for $\tan\theta \neq (2S+1)/(2R+1)$,

$$x = x_0 + \epsilon \Bigg[\frac{1024A}{\pi^6 \sin\alpha_0} \sum_{r=0}^{\infty} \sum_{s=0}^{\infty} (2r+1)^{-3}(2s+1)^{-3} \{(2s+1)^2\cos^2\theta - (2r+1)^2 \sin^2\theta\}^{-1}$$
$$\times \Bigg\{ \begin{pmatrix} -[(2r+1)^2+(2s+1)^2]\sin\theta\cos\theta \\ (2r+1)(2s+1) \end{pmatrix} \cos\frac{2\pi(2r+1)x_0^*}{a} \sin\frac{2\pi(2s+1)y_0^*}{a}$$
$$- \begin{pmatrix} (2r+1)(2s+1) \\ -[(2r+1)^2+(2s+1)^2]\sin\theta\cos\theta \end{pmatrix} \sin\frac{2\pi(2r+1)x_0^*}{a} \cos\frac{2\pi(2s+1)y_0^*}{a} \Bigg\}$$
$$- \frac{1024A}{\pi^6} \cot\alpha_0 \sum_{r=0}^{\infty} \sum_{s=0}^{\infty} (2r+1)^{-3}(2s+1)^{-3} \sin\frac{2\pi(2r+1)x_0^*}{a} \sin\frac{2\pi(2s+1)y_0^*}{a} \Bigg], \tag{4.29}$$

where the upper and lower terms are taken according to whether $(2s+1)/(2r+1)$ is less than or greater than $\tan\theta$. Should $\tan\theta = (2S+1)/(2R+1)$, where R and S are integers, then the expression (4.29) may still be used except that terms for which $(2s+1)/(2r+1) = \tan\theta$ are omitted from the first double summation and in their place an additional term

$$\epsilon \Bigg[\frac{512A}{\pi^6} \frac{\cot 2\theta}{\sin\alpha_0} (2R+1)^{-3}(2S+1)^{-3} \sum_{p=1}^{\infty} p^{-6} \sin\frac{2\pi p}{a} \{-(2R+1)x_0^* + (2S+1)y_0^*\} \Bigg]$$

is added. It is noted that the above results are qualitatively similar to those for example (i) except that there are now an infinite number of contact-line orientations for which there is contact-angle hysteresis, these orientations being determined by

$$\theta = \tan^{-1} \frac{2S+1}{2R+1}, \tag{4.30}$$

where R and S are integers $\geqslant 0$. In general it seems that the number of values of θ for which hysteresis occurs is determined by the number of non-zero Fourier coefficients present in (4.1). From (4.27) it is observed that for any value of θ satisfying (4.30) the contact angle β oscillates as x_0 is increased (see figure 10) yielding an advancing contact angle of

$$\beta_a = \alpha_0 + \frac{\epsilon A}{a} K \frac{[(2R+1)^2+(2S+1)^2]^{\frac{1}{2}}}{(2R+1)^3(2S+1)^3} \tag{4.31}$$

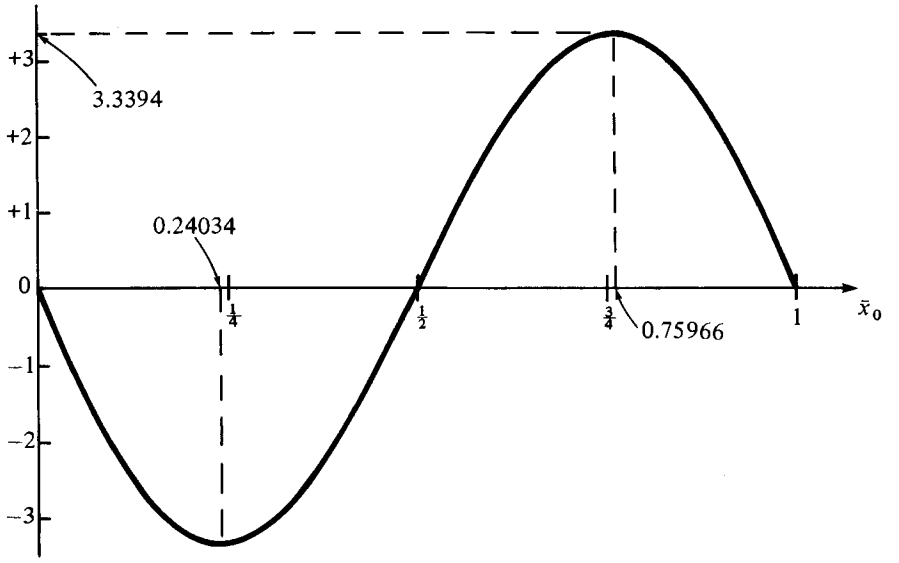

FIGURE 10. Value of

$$(\beta-\alpha_0)(2R+1)^3(2S+1)^3\Big/\frac{\epsilon A}{a}[(2R+1)^2+(2S+1)^2]^{\frac{1}{2}} \equiv \frac{2048}{15}\bar{x}(\bar{x}+\tfrac{1}{2})(\bar{x}-1)(\bar{x}^2-\bar{x}-\tfrac{1}{3})$$

as a function of $\bar{x}$ for $0 \leqslant \bar{x} \leqslant 1$ (see (4.27)).

and a receding contact angle of

$$\beta_r = \alpha_0 - \frac{\epsilon A}{a} K \frac{[(2R+1)^2+(2S+1)^2]^{\frac{1}{2}}}{(2R+1)^3(2S+1)^3}, \tag{4.32}$$

where

$$K = \frac{1024}{675}(3+\sqrt{30})\,[\tfrac{1}{60}(15-2\sqrt{30})]^{\frac{1}{2}} = 3.3394. \tag{4.33}$$

Values of θ, β_a and β_r are given for various values of R and S in table 1. Thus it is seen that while there is an infinite number of values of θ satisfying (4.30) in any small interval, the magnitude $\beta_a - \beta_r$ of the contact-angle hysteresis decreases very rapidly as R and S are increased. Thus the major effect of hysteresis will occur where the contact-line orientation is $\theta = \pm\frac{1}{4}\pi$.

For an advancing contact line with θ satisfying (4.30) the forward jumps of the contact line occur at

$$\bar{x}_0 = \tfrac{1}{2} + [\tfrac{1}{60}(15-2\sqrt{30})]^{\frac{1}{2}} + n' = 0.75955 + n', \tag{4.34}$$

while for a receding contact line, jumps occur at

$$\bar{x}_0 = \tfrac{1}{2} - [\tfrac{1}{60}(15-2\sqrt{30})]^{\frac{1}{2}} + n' = 0.24034 + n', \tag{4.35}$$

where $\bar{x}_0$ is defined by (4.28) and n' is any integer.

These contact line positions are shown in figure 11. It is observed that the angles given by (4.30) for which contact-angle hysteresis occurs are precisely those for which surface roughness is periodic along the contact line (with period $[(2R+1)^2+(2S+1)^2]^{\frac{1}{2}}a$). The values of this period together with the distance $a[(2R+1)^2+(2S+1)^2]^{-\frac{1}{2}}$ over which the contact line jumps occur are shown in table 1.

It may be noted in both examples (i) and (ii) that as θ approaches a value for which there is contact-angle hysteresis (at order ϵ^{+1}), the amplitude of the contact-line waviness tends to infinity. A similar result was obtained for the parallel grooved surface in §3.

(R, S)	θ given by (4.30)	$\frac{(\beta_a-\beta_r)/\epsilon A}{a}$ derived by (4.31) and (4.32)	Period/a $=[(2R+1)^2+(2S+1)^2]^{\frac{1}{2}}$	δ/a derived by (4.28)	$\Delta E_a^*/\epsilon\sigma A \sin\alpha_0$ given by (6.11)
(0,0)	45°	9.445	1.414	0.7071	3.339
(0,1)	18.43°	0.7822	3.162	0.3162	0.1237
(0,2)	11.31°	0.2724	5.099	0.1961	0.02672
(0,3)	8.13°	0.1377	7.071	0.1414	0.009736
(0,4)	6.34°	0.08296	9.055	0.1104	0.004581
(0,5)	5.19°	0.05542	11.045	0.09054	0.002509
(0,6)	4.40°	0.03964	13.04	0.07670	0.001520
(0,7)	3.81°	0.02975	15.03	0.06652	0.0009895
(0,8)	3.37°	0.02315	17.03	0.05872	0.0006797
(0,9)	3.01°	0.01853	19.03	0.05256	0.0004869
(0,10)	2.73°	0.01516	21.02	0.04757	0.0003606
etc.					
(1,1)	Included in (0,0)				
(1,2)	30.96°	0.01154	5.831	0.1715	0.0009895
(1,3)	23.20°	0.005492	7.616	0.1313	0.0003606
(1,4)	Included in (0,1)				
(1,5)	15.26°	0.002119	11.40	0.08771	0.00009292
(1,6)	12.99°	0.001502	13.34	0.07495	0.00005630
(1,7)	Included in (0,2)				
etc.					
(2,2)	Included in (0,0)				
(2,3)	35.54°	0.001340	8.602	0.1162	0.00007789
etc.					

TABLE 1. Details of contact-line jumps for spreading on a solid surface with elevation ζ given by (4.25). For each (R, S) values are given of the contact line orientation θ, the dimensionless contact-angle hysteresis $(\beta_a-\beta_r)/(\epsilon A/a)$, the dimensionless periodicity along the contact line, the dimensionless jump distance δ/a and the dimensionless energy release per jump $\Delta E_a^*/(\epsilon\sigma A \sin\alpha_0)$.

5. General rough surfaces

To investigate to what extent the results obtained in §§3 and 4 apply to spreading on a solid surface with a more general variation of surface elevation ζ, we will first express in an alternative form the value of the macroscopic contact angle β given by (3.14) for a surface with periodicity along the contact line (with ζ given by (3.1)). The Fourier coefficients $p_n(x)$, $q_n(x)$ in (3.14) may be obtained from (3.1) as

$$\left.\begin{aligned} p_n(x) &= \frac{2}{b}\int_0^b \zeta(x, y)\sin\frac{2\pi n y}{b}\,dy, \\ q_n(x) &= \frac{2}{b}\int_0^b \zeta(x, y)\cos\frac{2\pi n y}{b}\,dy \quad (n \geqslant 1), \\ q_0(x) &= \frac{1}{b}\int_0^b \zeta(x, y)\,dy. \end{aligned}\right\} \tag{5.1}$$

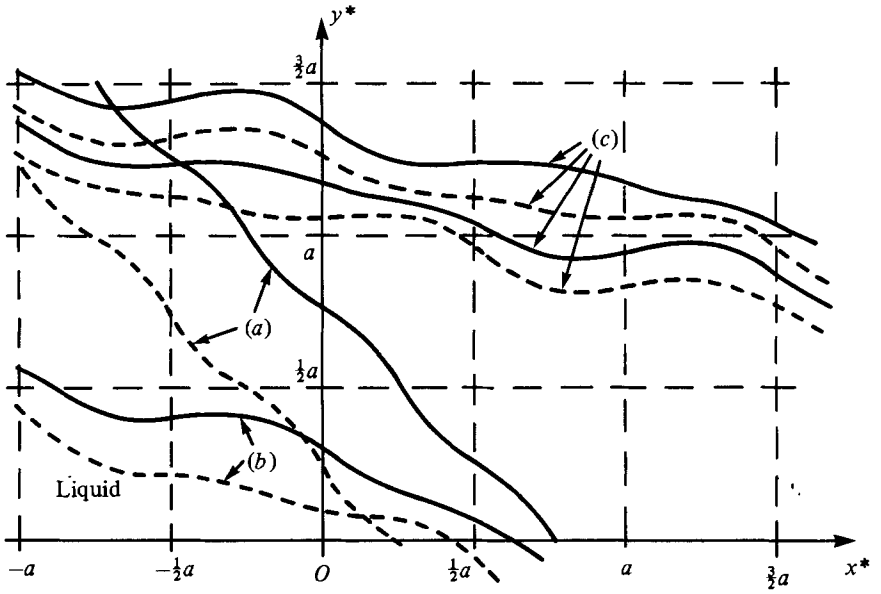

FIGURE 11. For spreading on a solid surface with dimensionless elevation ζ given by (4.25), the contact-line positions (projected in the (x^*, y^*)-plane) at which advancing jumps occur are shown by the continuous lines while those at which receding jumps occur are shown by broken lines. $\epsilon A/a$ has been chosen to be 0.025 with $\alpha_0 = 30°$ (as for the situation shown in figure 8). For the curves denoted by (a), $(R, S) = (0, 0)$, while for (b), $(R, S) = (0, 1)$ and for (c), $(R, S) = (0, 2)$.

Then, by direct substitution of these values, we obtain

$$\sum_{n=1}^{\infty} [\{p_n'(x_0, y)\}^2 + \{q_n'(x_0, y)\}^2]$$
$$= \sum_{n=1}^{\infty} \frac{4}{b^2} \int_0^b \int_0^b \frac{\partial \zeta}{\partial x}(x_0, y) \frac{\partial \zeta}{\partial x}(x_0, y^*) \cos \frac{2\pi n(y-y^*)}{b} \, dy \, dy^*$$
$$= 2\left(\overline{\frac{\partial \zeta}{\partial x}\bigg|_{x=x_0}} - \frac{\overline{\partial \zeta}}{\partial x}\bigg|_{x=x_0} \right)^2, \tag{5.2}$$

where the summation has been done using the result

$$\sum_{n=1}^{\infty} \cos n\lambda = -\tfrac{1}{2} + \pi\delta(\lambda) \quad (-\pi < \lambda < \pi). \tag{5.3}$$

The bar over symbols in (5.2) denotes the average value with respect to y over one period on the mean contact line $x = x_0$. In a similar manner the various other terms appearing in (3.14) may be obtained as

$$\sum_{n=1}^{\infty} n^2(p_n^2 + q_n^2) = \frac{b^2}{2\pi^2} \overline{\left(\frac{\partial \zeta}{\partial y}\bigg|_{x=x_0} \right)^2}, \tag{5.4}$$

$$\sum_{n=1}^{\infty} (p_n p_n'' + q_n q_n'') = \overline{2\zeta|_{x=x_0} \frac{\partial^2 \zeta}{\partial x^2}\bigg|_{x=x_0}} - 2\overline{\zeta}|_{x=x_0} \overline{\frac{\partial^2 \zeta}{\partial x^2}\bigg|_{x=x_0}}, \tag{5.5}$$

$$q_0 = \overline{\zeta|_{x=x_0}}, \quad q_0'' = \overline{\frac{\partial^2 \zeta}{\partial x^2}\bigg|_{x=x_0}}, \tag{5.6}$$

$$\sum_{n=1}^{\infty} n^{-1}(p_n' p_n'' + q_n' q_n'') = -\frac{2}{b} \int_{u=-\frac{1}{2}b}^{+\frac{1}{2}b} \frac{\partial h(u, x_0)}{\partial x_0} \ln\left(2\left| \sin \frac{\pi u}{b} \right| \right) du \tag{5.7}$$

where $h(u, x_0)$ is the surface-slope correlation

$$h(u, x_0) = \overline{\frac{\partial \zeta}{\partial x}(x_0, y)\frac{\partial \zeta}{\partial x}(x_0, y+u)}. \tag{5.8}$$

In deriving (5.7), we have made use of the result

$$\sum_{n=1}^{\infty} \frac{\cos n\lambda}{n} = -\ln(2|\sin \tfrac{1}{2}\lambda|) \quad (-\pi < \lambda < \pi). \tag{5.9}$$

Substituting the values given by (5.2) and (5.4)–(5.7) into (3.14) we obtain an alternative expression for the macroscopic contact angle as

$$\beta = \alpha_0 - \epsilon\overline{\frac{\partial \zeta}{\partial x}} + \epsilon^2\left[\tfrac{1}{2}\cot\alpha_0\overline{\left(\frac{\partial \zeta}{\partial x} - \overline{\frac{\partial \zeta}{\partial x}}\right)^2} + \cot\alpha_0\,\overline{\zeta\frac{\partial^2 \zeta}{\partial x^2}} - \tfrac{1}{2}\cot\alpha_0\overline{\left(\frac{\partial \zeta}{\partial y}\right)^2}\right.$$
$$\left. + \frac{1}{2\pi\sin\alpha_0}\int_{-\frac{1}{2}b}^{+\frac{1}{2}b}\frac{\partial h(u, x_0)}{\partial x_0}\ln\left(2\left|\sin\frac{\pi u}{b}\right|\right)du\right] + O(\epsilon^3), \tag{5.10}$$

where all quantitites are evaluated on the mean contact-line position $x = x_0$. In order to determine the value of β for a rough solid surface that does not show any periodicity along the contact line, we shall consider the limit of the period b tending to infinity. Thus it is necessary to obtain the asymptotic form for $b \to \infty$ of the integral

$$I = \int_{-\frac{1}{2}b}^{+\frac{1}{2}b}\frac{\partial h(u, x_0)}{\partial x_0}\ln\left(2\left|\sin\frac{\pi u}{b}\right|\right)du \tag{5.11}$$

appearing in (5.10).

For this purpose, we define a new slope-correlation function $h^*(u, x_0)$ as

$$h^*(u, x_0) = \overline{\left\{\frac{\partial \zeta}{\partial x}(x_0, y) - \overline{\frac{\partial \zeta}{\partial x}}\right\}\left\{\frac{\partial \zeta}{\partial x}(x_0, y+u) - \overline{\frac{\partial \zeta}{\partial x}}\right\}}, \tag{5.12}$$

which may be written alternatively as

$$h^*(u, x_0) = h(u, x_0) - \overline{\left(\frac{\partial \zeta}{\partial x}\right)^2}. \tag{5.13}$$

By direct substitution of $h^*(u, x_0)$, we may show that

$$\int_{-\frac{1}{2}b}^{+\frac{1}{2}b} h^*(u, x_0)\,du = 0, \tag{5.14}$$

while, by contour integration, we obtain

$$\int_{-\frac{1}{2}b}^{+\frac{1}{2}b}\ln\left(2\left|\sin\frac{\pi u}{b}\right|\right)du = 0.$$

In addition, it follows from the definition (5.12) that

$$h^*(-u, x_0) = h^*(+u, x_0). \tag{5.16}$$

The integral I in (5.11) may now be manipulated using the results (5.13)–(5.16) to give

$$I = 2\frac{\partial}{\partial x_0}\int_0^{\frac{1}{2}b} h^*(u, x_0)\ln\left(\frac{b}{\pi}\sin\frac{\pi u}{b}\right)du, \tag{5.17}$$

which in the limit of $b \to \infty$ gives

$$\lim_{b\to\infty} I = 2\frac{\partial}{\partial x_0}\int_0^{\infty} h^*(u, x_0)\ln u\,du. \tag{5.18}$$

It has been assumed here that as $u \to \infty$, the slope correlation $h^*(u, x_0)$ tends to zero sufficiently fast to make the integral in (5.18) convergent. Assuming that this is the case, then for a general rough surface with no periodicity along the mean contact line, the results (5.10) for the macroscopic contact angle β reduces to

$$\beta = \alpha_0 - \epsilon \overline{\frac{\partial \zeta}{\partial x}} + \epsilon^2 \left[\tfrac{1}{2} \cot \alpha_0 \overline{\left(\frac{\partial \zeta}{\partial x} - \overline{\frac{\partial \zeta}{\partial x}} \right)^2} + \cot \alpha_0 \overline{\zeta \frac{\partial^2 \zeta}{\partial x^2}} \right.$$
$$\left. - \tfrac{1}{2} \cot \alpha_0 \overline{\left(\frac{\partial \zeta}{\partial y} \right)^2} + \frac{1}{\pi \sin \alpha_0} \frac{\partial}{\partial x} \int_0^\infty h^*(u, x) \ln u \, du \right] + O(\epsilon^3), \quad (5.19)$$

where all quantities are evaluated at the mean contact-line position $x = x_0$. It may be shown that

$$\overline{\frac{\partial \zeta}{\partial x}} = \frac{\partial \bar{\zeta}}{\partial x},$$
$$\overline{\left(\frac{\partial \zeta}{\partial x} - \overline{\frac{\partial \zeta}{\partial x}} \right)^2} = \overline{\left(\frac{\partial \zeta}{\partial x} \right)^2} - \left(\frac{\partial \bar{\zeta}}{\partial x} \right)^2,$$
$$\overline{\zeta \frac{\partial^2 \zeta}{\partial x^2}} = \frac{1}{2} \frac{\partial^2}{\partial x^2} \overline{\zeta^2} - \overline{\left(\frac{\partial \zeta}{\partial x} \right)^2},$$

so that (5.19) may be written as

$$\beta = \alpha_0 - \epsilon \frac{\partial}{\partial x} \bar{\zeta} + \epsilon^2 \left[\tfrac{1}{2} \cot \alpha_0 \left\{ - \overline{\left(\frac{\partial \zeta}{\partial x} \right)^2} - \overline{\left(\frac{\partial \zeta}{\partial y} \right)^2} - \left(\frac{\partial \bar{\zeta}}{\partial x} \right)^2 + \frac{\partial^2}{\partial x^2} \overline{\zeta^2} \right\} \right.$$
$$\left. + \frac{1}{\pi \sin \alpha_0} \frac{\partial}{\partial x} \int_0^\infty h^*(u, x) \ln u \, du \right] + O(\epsilon^2). \quad (5.20)$$

Should the solid surface be homogeneous in the sense that statistical properties of ζ are independent of position (i.e. $\bar{\zeta}$, $\overline{\zeta^2}$ and $h^*(u, x)$ are independent of x) then β is given by

$$\beta = \alpha_0 - \epsilon^2 \tfrac{1}{2} \cot \alpha_0 \left\{ \overline{\left(\frac{\partial \zeta}{\partial x} \right)^2} + \overline{\left(\frac{\partial \zeta}{\partial y} \right)^2} \right\}, \quad (5.21)$$

which, being independent of x_0, indicates no contact-angle hysteresis for spreading on such a surface. However, care must be used in interpreting this result since this lack of contact-angle hysteresis may result from the implicit assumption used in the theory that the deviation of the contact line from its mean straight-line position is everywhere very much smaller than the roughness wavelength. This assumption was necessary in order to make Taylor expansions of the boundary conditions. Further investigation is required to resolve the question as to whether the removal of this assumption results in the prediction of contact-angle hysteresis. It is noted, however, that the surface roughness causes, on the basis of the present theory, a change of contact angle from the value α_0 by an amount $O(\epsilon^2)$, with β being smaller or larger than α_0 according to whether α_0 is less than or greater than $\frac{1}{2}\pi$.

6. Comparison with Wenzel's equation

If, for the spreading of a liquid on a rough solid surface, it is assumed that there is no contact-angle hysteresis, so that the macroscopic contact angle, β^* say, is a constant, then it has been shown by Wenzel (1936) that β^* is related to α_0 by the relation

$$\cos \beta^* = \frac{A_s}{A_p} \cos \alpha_0, \quad (6.1)$$

where A_s is the actual area of the solid surface and A_p its projected area on the (x, y)-plane. This relation was derived by considering a small advance of the liquid interface and by equating the work done by the liquid–air interfacial tension to the increase of surface energy of the system. For rough surfaces with small slope angles of order ϵ considered in this paper this result (6.1) takes the form

$$\beta^* = \alpha_0 - \epsilon^2 \tfrac{1}{2} \cot \alpha_0 \left\langle \left(\frac{\partial \zeta}{\partial x}\right)^2 + \left(\frac{\partial \zeta}{\partial y}\right)^2 \right\rangle \tag{6.2}$$

where the angle brackets $\langle\ \rangle$ denote an area average. For a homogeneous general random surface this result is identical with (5.21). In addition (6.2) may also be shown to agree with the value of β given by (3.20) for a parallel grooved surface (with $\theta \neq 0$) and with the value of β given by (4.7) for a doubly periodic surface (for which $\tan \theta \neq Na/Mb$ and $\theta \neq 0, \frac{1}{2}\pi$). Thus in all cases we have considered for which there is no contact-angle hysteresis, the results obtained agree, as they should, with Wenzel's equation (6.1). However, when hysteresis is predicted, the values of the advancing and receding contact angles will be different from the value of β^* given by (6.1). Thus for an advancing contact angle of β_a, if the contact line (over a given part of its length) advances over a projected area A_p then the work done by the interfacial tension σ of the liquid–air interface is $-\sigma A_p \cos \beta_a$. The corresponding increase in the surface energy of the system is then $(\sigma_{SL} - \sigma_{SA}) A_S$, where σ_{SL} and σ_{SA} are respectively the surface energies per unit area of the solid–liquid and solid–air interfaces. The excess work ΔE_a done on the system is thus

$$\Delta E_a = -\sigma A_p \cos \beta_a - (\sigma_{SL} - \sigma_{SA}) A_S. \tag{6.3}$$

When there is no hysteresis, so that the contact angle is β^* given by (6.1), the value of ΔE_a is zero, whence

$$0 = -\sigma A_p \cos \beta^* - (\sigma_{SL} - \sigma_{SA}) A_S. \tag{6.4}$$

Thus

$$\Delta E_a = \sigma A_p (\cos \beta^* - \cos \beta_a), \tag{6.5}$$

which being strictly positive implies that $\beta_a > \beta^*$. Similarly for a receding contact line the excess work ΔE_r done is

$$\Delta E_r = \sigma A_p (\cos \beta_r - \cos \beta^*), \tag{6.6}$$

where β_r is the receding contact angle. This quantity ΔE_r being strictly positive implies that $\beta^* > \beta_r$. For rough surfaces of small slope angle ϵ, since the values of β^*, β_a, β_r and α_0 only differ by a small amount, (6.5) and (6.6) may be written as

$$\Delta E_a = \sigma A_p (\beta_a - \beta^*) \sin \alpha_0, \tag{6.7}$$

$$\Delta E_r = \sigma A_p (\beta^* - \beta_r) \sin \alpha_0. \tag{6.8}$$

For both advancing and receding contact lines, this excess energy ΔE is lost during the jumping of the contact line, which is a dynamic process in which the motion of the liquid is important. Thus this energy may be (i) radiated away as a capillary wave along the liquid–air surface and/or (ii) converted to heat by viscous dissipation in the liquid (see Huh & Mason 1977*a*). If the length of a contact-line jump is δ then the energy ΔE^* released per unit length of contact line in a single jump is, for an advancing contact line,

$$\Delta E_a^* = \sigma \delta (\beta_a - \beta^*) \sin \alpha_0, \tag{6.9}$$

and, for a receding contact line,

$$\Delta E_r^* = \sigma \delta (\beta^* - \beta_r) \sin \alpha_0. \tag{6.10}$$

As an example, consider the doubly periodic surface described by (4.23) and (4.24) (i.e. example (ii) of §4) with $\tan\theta = (2S+1)/(2R+1)$, so that there is contact-angle hysteresis. Then from the results (4.31)–(4.33), it is seen that

$$\Delta E_{\mathrm{a}}^{*} = \Delta E_{\mathrm{r}}^{*} = 3.3394 \frac{\epsilon\sigma A \sin\alpha_0}{(2R+1)^3 (2S+1)^3}. \tag{6.11}$$

The value of this amount of energy released in a jump (listed in table 1) very rapidly decreases as the values of the integers R and S are increased.

7. Conclusions

For the slow spreading of a liquid on a solid surface, we have investigated the effect that roughness of the surface has on the macroscopic contact angle. In order to do this, it was assumed that (i) the value of the microscopic contact angle α_0 was everywhere constant and (ii) the characteristic slope of the surface roughness ϵ was small.

It was found for spreading on a parallel grooved surface with the contact line parallel to the grooves that the macroscopic contact angle would oscillate by an amount of order ϵ as the contact line advanced. This indicates that contact-angle hysteresis (of order ϵ) and stick–jump behaviour of the contact line can be expected. However, for contact lines in all other directions, no such phenomenon occurs, so that no hysteresis or stick–jump behaviour would be evident. Thus it would be expected that an expanding drop on a parallel grooved surface would not be able to spread so well in the direction perpendicular to the grooves (where the contact line is parallel to the groove direction). Hence the drop perimeter will be flattened at such positions. In fact, drops of such a shape have been observed on parallel grooved surfaces by Oliver *et al.* (1977).

For spreading on a doubly periodic rough surface there are in general an infinite number of contact-line directions (with $\theta = \pm\tan^{-1}(Na/Mb)$, where N and M are integers) for which there is contact-angle hysteresis (of order ϵ) with all other contact-line directions showing no hysteresis at all. The larger the values of N and M, the smaller will be the corresponding contact-angle hysteresis. However, for special doubly periodic surfaces for which the number of Fourier coefficients is finite, the number of contact-line orientations for which there is hysteresis is also finite.

For the above examples it was observed that for any given equilibrium position of the contact line the positions of maximum contact-line advance tend to occur in regions where the surface elevation is a minimum (for $\alpha_0 < \frac{1}{2}\pi$) and/or the regions where the surface upslope (from liquid to air) normal to the contact line is a maximum.

By considering a periodic rough surface and letting its period tend to infinity, we obtained results for spreading on a general non-periodic rough surface. These indicated no contact-angle hysteresis on such a surface. However, this conclusion may merely result from an implicit assumption made in the theory that the deviation of the contact line from its mean straight-line position is everywhere very much smaller than the roughness wavelength. Thus, while contact-angle hysteresis is predicted (at least for some contact-line orientations) for spreading on periodic surfaces, the existence and nature of possible hysteresis on more general surface roughness has yet to be established.

It was noted that in all cases where there was no contact-angle hysteresis, the value of the predicted macroscopic contact angle was different from α_0 by an amount which

is determined by Wenzel's (1936) equation. For situations where there is contact-angle hysteresis, the amount of energy liberated during a single contact-line jump was calculated.

While in this paper we have, for convenience, considered the movement of a liquid–air interface across a rough solid surface, all results will of course apply to the movement of any liquid–fluid interface across a rough solid surface.

Finally it should be pointed out that, for a drop of volume R^3 resting on a rough surface, a change in macroscopic contact angle of order ϵ (corresponding to the possible variations in β due to hysteresis, as predicted for the doubly periodic rough surface) would cause a change in contact-line position of order ϵR. For many possible equilibrium positions to exist, there must be many roughness wavelengths in this distance ϵR (since for any β, the distance between equilibrium contact-line positions is of the order of the roughness wavelength). Thus for many possible equilibrium positions of the drop, we require

$$\epsilon R \gg l. \tag{7.1}$$

As mentioned in §1, this condition was violated by Huh & Mason (1977*a*), who considered $\epsilon \to 0$ with l/R fixed. This explains why they failed to obtain multiple equilibrium positions.

This work was supported by the National Sciences and Engineering Research Council of Canada under Grant A7007.

REFERENCES

Bascom, W. D., Cottington, R. L. & Singleterry, C. R. 1964 *Adv. Chem.* **43**, 355.
Bikerman, J. J. 1950 *J. Phys. Chem.* **54**, 653.
Dussan, V., E. B. 1979 *Ann. Rev. Fluid Mech.* **11**, 371.
Dussan, V., E. B. & Davis, S. H. 1974 *J. Fluid Mech.* **65**, 71.
Hocking, L. M. 1976 *J. Fluid Mech.* **76**, 801.
Hocking, L. M. 1977 *J. Fluid Mech.* **79**, 209.
Huh, C. & Mason, S. G. 1977*a* *J. Colloid Interface Sci.* **60**, 11.
Huh, C. & Mason, S. G. 1977*b* *J. Fluid Mech.* **81**, 401.
Johnson, E. R. & Dettre, R. H. 1964 *Adv. Chem.* **43**, 112.
Oliver, J. F., Huh, C. & Mason, S. G. 1977 *J. Adhesion* **8**, 223.
Oliver, J. F. & Mason, S. G. 1977 *J. Colloid Interface Sci.* **60**, 480.
Parker, E. R. & Smoluchowski, R. 1945 *Trans. Am. Soc. Metals* **35**, 362.
Schwartz, A. M. 1980 *J. Colloid Interface Sci.* **75**, 404.
Trillat, J. & Fritz, R. 1938 *J. Chim. Phys.* **35**, 45.
Wenzel, R. N. 1936 *Ind. Engng Chem.* **28**, 988.